

Assessing the Intervertebral Disc via gagCEST

W. Ling¹, G. Saar², R. R. Regatte³, A. Jerschow⁴, and G. Navon²

¹CMRR, Univ. of Minnesota, Minneapolis, MN, United States, ²School of Chem., Tel Aviv Univ., Ramat Aviv, Tel Aviv, Israel, ³Dept. of Radiology, NYU, New York, NY, United States, ⁴Chem. Dept., NYU, NY, United States

Introduction: Disc degeneration is an irreversible process of an aberrant, cell-mediated response to progressive structure failure, which results in loss of proteoglycans (PG) and the reduction of the osmotic pressure. As a consequence the strength of the disc is weakened and a shrinkage of the disc height is observed. Thus the diagnostics of early degenerative changes at the stage of PG loss in structurally sound disc is vital for preventing the disease from compromising life quality since the chronic accumulation of the change in morphology is hard to restore^{1,2}. Current clinical protocols assess disc degeneration includes $T_{1\rho}$ relaxometry and ^{23}Na MRI. $T_{1\rho}$ relaxometry is not strictly specific for PG and the high specific absorption rate (SAR) hampers its wide application³. ^{23}Na MRI use the concentration of positively charged ^{23}Na in cartilage to map the negatively charged PG⁴. The low signal-to-noise ratio and the requirement of special hardware, however, currently limit its clinical application. We recently proposed to assess glycosaminoglycan concentration via the Chemical Exchange Saturation Transfer (gagCEST) approach in cartilage^{5,6}. Here we demonstrate that the gagCEST method can be extended to map PG concentration in intervertebral disc.

Materials and Methods

NMR experiments: The bovine disc samples were cut so as to include only the anatomical region of interest, i.e. the annulus fibrosus (AF) and the nucleus pulposus (NP), separately, and placed into 5 mm NMR tubes. Both ^1H and ^{23}Na data were acquired at 11.7 T using a Bruker Avance spectrometer with a BBO probe. A 5° pulse flip angle with $\omega_1/2\pi = 23\text{kHz}$ was used, and 8 transients were acquired for each spectrum using a repetition delay of 1 s. In the CEST experiments The CW wave power for saturation was 50 Hz and the duration 10 s.

MRI experiments: The porcine disc samples were cut so as to include every anatomical region of disc, and placed into a plastic jar. Data were acquired at Bruker 7 T using a 7 cm Birdcage coil. For both anatomical imaging and CEST imaging, a spoil gradient GRE sequence with 30° flip angles. The acquisition parameters of the image on the disc were: TR/TE = 3050/3.5 ms; thickness = 1.8 mm; acquisition matrix = 256x256; FOV = 45 mm x 45 mm. The CEST imaging sequence was acquired with the spoil gradient GRE sequence with a train of thirty pulses of 100 ms duration each and an interval of 1 ms at the offsets ± 1.0 ppm. The average saturation power was 1.8 μT . The T_1 map was generated by a multi-slice multiecho (MSME) sequence with only 1 echo. TE was 12ms in all 8 experiments and TR was set to 100ms, 200ms, 400ms, 600ms, 1000ms, 1500ms, 2000ms, 8000ms, respectively. 2 dummy scans were used to achieve a steady state. Two averages were accumulated. The T_2 map was generated by MSME sequence with 32 echoes on a single slice. No dummy scans were used. Two averages were accumulated.

Results & Discussion: Figure 1a and 1b shows 1D ^1H spectroscopy of both AF and NP tissue from bovine IVDs. The most prominent peaks include lipids (between -3.2 ppm and -4.0 ppm), N-acetyl group from GAG (-2.7 ppm), aliphatic proton from GAG ring (between -0.6ppm to 1.4 ppm), amide proton from GAG (+3.2ppm), and amine groups from the sidechains of proteoglycan core protein (+2.9 ppm). In order to demonstrate the CEST effect on IVDs, a z-spectrum is constructed on both AF and NP samples. In these spectra, the exchangeable groups and sites which show a magnetization transfer through the nuclear Overhauser effect (NOE)⁶ are both visible as dips or bents in the curve, making it asymmetric.

Figure 2d, 2e, and 2f show axial images of an ex vivo intact porcine IVD, including image at -1.0ppm image (Figure 2a), +1.0ppm image (Figure 2b), and CEST image (Figure 2c) extracted according to

$$\text{CEST}(1.0\text{ppm}) = [M_{\text{sat}}(-1.0\text{ppm}) - M_{\text{sat}}(+1.0\text{ppm})] / M_{\text{sat}}(-1.0\text{ppm})$$

Eqn [1].

the gagCEST demonstrates robust contrast in both AF and NP region. Its contrast in NP is about ~65 %, while it is ~40% in AF. Although the anatomical image in Figure 2a shows clear structural differences in AF and NP, little information is provided about GAG distribution. Table lists the extracted CEST contrast, and its corresponding T_1 , T_2 , and GAG concentration in corresponding region of IVD. The stronger CEST effect from NP is due to: (i) the GAG concentration in NP is up to 50% by dry weight (~350 mM GAG in healthy disc NP and 200 mM in AF); (ii) the CEST effect itself increases with increasing T_1 of the bulk water.

	CEST	$T_1/\text{sec.}$	T_2/ms	Sensitivity/
Outer AF	25 \pm 4%	0.7 \pm 0.3	19.1 \pm 8.4	29%
Inner AF	48 \pm 8%	1.3 \pm 0.4	32.3 \pm 6.2	28%
NP	68 \pm 5%	3.0 \pm 0.4	109.2 \pm 2.8	36%

Conclusion: We show here that the exchangeable protons from the -OH groups of GAG can be used in a CEST method to measure the concentration of GAG in intervertebral disc tissue. The high concentration of GAG and the longer T_1 of water, make the method sensitive, in particular for assessing the nucleus pulposus. The CEST effect in NP is about 1.5 times stronger than that of AF. In disc degeneration, the loss of GAG is mainly manifested in NP while little change is visible in AF. gagCEST hold great potential for future MRI methodology development MRI for the assessment of disc pathophysiology.

- Adams, M. A.; Roughley, P. J. *Spine* **2006**, 31, 2151-2161.
- Urban, J. P. G.; Winlove, C. P. *Journal of Magnetic Resonance Imaging* **2007**, 25, 419-432.
- Blumenkrantz, G.; Li, X.; Han, E. T.; Newitt, D. C.; Crane, J. C.; Link, T. M.; Majumdar, S. *Magnetic Resonance Imaging* **2006**, 24, 1001-1007.
- Lesperance, L. M.; Gray, M. L.; Burstein, D. *Journal of Orthopaedic Research* **1992**, 10, 1-13.
- Ling, W.; Regatte, R. R.; Schweitzer, M. E.; Jerschow, A. *NMR in Biomedicine* **2008**, 21, 289-295.
- Ling, W.; Regatte, R. R.; Navon, G.; Jerschow, A. *Proceedings of the National Academy of Sciences* **2008**, 105, 2266-2270.
- Abraham, A. *Principles of Nuclear Magnetism*, 1961.

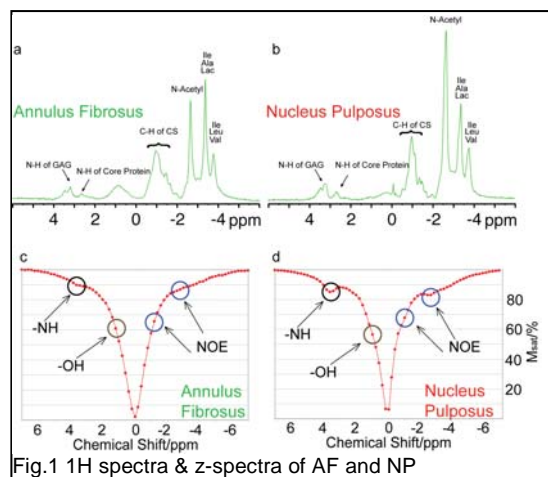


Fig.1 1H spectra & z-spectra of AF and NP

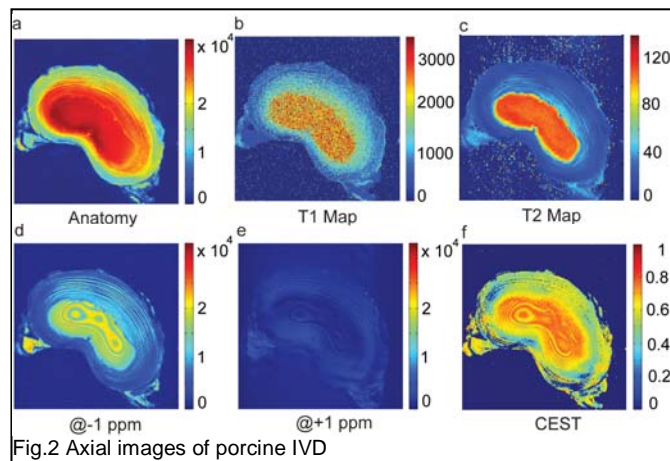


Fig.2 Axial images of porcine IVD